Effect of organic friction modifiers on lubrication of PEEK-steel contact

Go Tatsumi[1), 2) *], Monica Ratoi[1)], Yuji Shitara[2)], Kiyomi Sakamoto[2)], Brian G. Mellor[3)]

1) National Centre for Advanced Tribology at Southampton (nCATS), University of Southampton, Southampton SO17 1BJ, United Kingdom

2) Lubricants R&D Dept., JXTG Nippon Oil & Energy Corporation, 8, Chidoricho, Naka-ku, Yokohama 231-0815, Japan

3) Faculty of Engineering and Physical Sciences, University of Southampton, Southampton SO17 1BJ, United Kingdom

*Corresponding author: tatsumi.go@jxtg.com

Abstract

The rapid adoption of the advantageous PEEK/steel pairing in many tribological applications has prompted intense research to optimize its lubrication. Thus, the role of organic friction modifiers (OFMs) in improving the lubrication of PEEK-steel contacts has been studied and their mechanism explained. Their effect on friction and wear depends on the type of contact motion (i.e. sliding or sliding-rolling) and the steel surface roughness. N-oleoyl sarcosine had a significant effect on tribological properties due to its ability to absorb strongly on both materials, inhibit the formation of PEEK transfer films on steel and thus exert either a positive or negative effect depending on the test conditions.

Keywords

Polyetheretherketone (PEEK), Organic friction modifiers (OFMs), Mixed and boundary lubrication, Sliding and sliding-rolling

1. Introduction

Polymers and polymer-based composites are becoming preferred materials in many tribological applications. Compared with metals, polymer materials have advantages such as lightweight, reduced noise and self-lubricating properties which make their use in automotive, aerospace, medical, industrial applications highly desirable [1–5]. On the other hand, the mechanical strength and thermal stability of polymers are lower than those of metals, and therefore they tend to suffer from failures such as wear, local melting and pitting when used under severe conditions [6–9]. Among the many types of polymers, Poly-Ether-Ether-Ketone (PEEK) has superior mechanical properties and higher thermal stability than other conventional polymers which make it suitable for tribological applications operating under severe conditions. [1–3,10,11]. Due to its self-lubricating properties in practice PEEK is commonly used with steel counterparts in dry conditions, and numerous studies have investigated the friction and wear properties of PEEK-steel contacts in dry conditions [12–19]. While there have been many attempts to improve the tribological performance of PEEK from the material side, as in the case of PEEK composites with specific fillers [20–26], fluid lubrication has the potential to further reduce friction and wear of PEEK [27–34]. However, the reports on the tribological performance of PEEK in lubricated conditions are scant and the effect and working mechanism of lubrication were not fully investigated, especially for the case with lubricant additives.

Lubricant additives are commonly added to base oil in small proportions to improve the lubricity and lifespan [35–37]. While there are various types of lubricant additives depending on their use, organic friction modifiers (OFMs) are historically some of the most essential lubricant additives [38,39]. OFMs are surfactant-like molecules generally consisting of long hydrocarbon chains (usually more than 10 carbon atoms) with polar groups (e.g. alcohol, amine, amide and carboxylic acid groups) at their ends. The effect of OFMs have been extensively investigated in steel-steel contacts [40–44], and the working mechanism proposed was that OFMs adsorb or chemically react on the polar steel surfaces to form dense monolayers or thick reacted viscous layers, thus preventing direct contact between two sliding surfaces and mitigating friction and wear. As PEEK contains the polar ketone group in the monomer structure, OFMs might absorb on the polar PEEK surfaces and improve further their tribological performances. Nevertheless, there has been little work reported about the effect of OFMs on lubrication of PEEK.

When trying to elucidate the effect and working mechanism of OFMs, there are two important factors to consider which are reported to influence the tribological properties of PEEK-steel contacts under lubrication: changes in hardness of PEEK surfaces and formation of PEEK transfer films on steel counterparts. Yamamoto and Takashima [45] showed that water lubrication of a PEEK-steel contact increased the wear of PEEK dramatically compared with the dry condition. Because the hardness of the PEEK sliding surface decreased in water lubrication, while the mere immersion in water did not lead to any changes, the authors postulated that the high wear of PEEK was caused by the softening of the rubbing surface during water lubrication. Similar softening of PEEK in water lubricated conditions was reported by Yamaguchi and Hokkirigawa [46]. Briscoe et al. [47] showed that chemicals such as decanoic acid and dodecyl amine (whose hydrocarbon chains are too short to work as OFMs) added to dodecane produced the softening of PEEK surfaces, causing a premature form of scuffing failure in the PEEK-steel contact.

Another key factor is the PEEK transfer films on steel counterparts which act as protective layers avoiding the direct contacts of PEEK surfaces with the hard asperities of steel counterparts [14,18,48]. Kurdi et al. [49] reported that water lubrication of a PEEK-steel contact reduced friction, but dramatically increased the wear of PEEK compared with dry

conditions. As a PEEK transfer film on the steel counterpart was not observed in water lubricated conditions, the authors concluded that water lubrication inhibits the formation of stable transfer films on steel counterparts. Tatsumi et al. [31] showed that lubrication with a poly-α-olefin (PAO) base oil suppressed not only the formation but also the removal of PEEK transfer films in the PEEK-steel contact, therefore causing either a positive or negative effect on wear of PEEK depending on the tribological test conditions.

The current study aimed to investigate the effect of OFMs on the lubrication of PEEK-steel contacts, and thus elucidate their working mechanism, essential to formulating optimal lubricants and developing ideally suited PEEK-based systems for tribological applications. This was achieved by focusing on two important factors influencing tribological properties, the hardness of PEEK surfaces and the PEEK transfer films on steel counterparts after tribological testing. The friction and wear properties of PEEK with steel counterparts were studied under lubrication with OFMs added to a PAO base oil in sliding and sliding-rolling contacts as encountered in tribological applications such as bushings, seals, gears and bearings, where lubricated PEEK-steel contacts are envisaged.

2. Experimental Methods

2.1. Materials

PEEK specimens for tribological tests were prepared as plates and balls. PEEK plates were injection molded from commercially available PEEK (Solvay® KT-820 NT). PEEK balls (Ketron® 1000) were purchased and drilled to fit the test rig. The Ra surface roughness of PEEK specimens was approximately 0.05 μm for plates and 0.1 μm for balls, respectively. They were used without polishing. Steel balls and discs (AISI 52100) were obtained from PCS Instruments Ltd. These steel specimens were with smooth surfaces of Ra = 0.01-0.02 μm. For tribological measurements under more severe conditions, rough steel balls were prepared from smooth balls by shot blasting to the Ra roughness of approximately 0.5 μm. New plates and balls were used for each test and cleaned with a hydrocarbon-mix solvent (FASTCLEAN 201, CRC Industries UK Ltd) and isopropanol prior to the test.

Three types of OFMs, oleylamine (OFM-A), oleic acid (OFM-B) and N-oleoyl sarcosine (OFM-C), were investigated in this study. The chemical structures of these OFMs are shown in **Fig. 1**. They have similar types of hydrocarbon moieties, but different polar groups. OFMs in this study were technical-grade, and contained a small amount of different hydrocarbon structures as impurities. However, the compositions of hydrocarbon structures were similar in the three OFMs, hence the main components of the effect of the OFMs were their polar groups.

Test oil formulations are listed in **Table 1**. The OFMs were added at 0.01 to 1.0 wt.% to a PAO base oil with a density of 0.819 g/cm^3 and viscosity of 17.5 cSt at 40 °C and 3.9 cSt at 100 °C (~31 cSt at 25 °C).

2.2. Tribological tests

Tribological tests were carried out at ambient temperature (approximately 25 °C) using a Mini Traction Machine (MTM) from PCS Instruments Ltd. in three configurations, PEEK-steel, PEEK-PEEK and steel-steel, as shown in **Fig. 2**. This study mainly focused on the PEEK-steel contact using a pair of a steel ball and a PEEK plate which was placed on top of a bespoke MTM disc and secured in place with the nut. In the PEEK-PEEK and steel-steel contacts, a PEEK ball and plate and a steel ball and plate respectively were used. Tribological tests were performed under two different

types of contact motion: sliding and sliding-rolling. In the sliding condition, the ball was kept stationary and only the disc was rotated. In the sliding-rolling condition, the ball and disc were driven independently to create a mixed sliding-rolling contact with the slide-roll ratio (SRR) of 50%. SRR is defined as the ratio of the sliding speed (u_d - u_b) to the entrainment speed ((u_d + u_b)/2), where u_d and u_b are the speeds of the disc and the ball with respect to the contact. In the sliding condition SRR is calculated as 200%. The entrainment speed was gradually increased up to 1 m/s and was maintained for 60 seconds at each speed. To allow for run-in, this speed cycle was repeated three times consecutively as shown in **Fig. 3**. The friction coefficients for the Stribeck curves were averaged over the last 20 seconds at each entrainment speed during the 3rd cycle. The applied loads were 50 N for the PEEK-steel and PEEK-PEEK contacts, and 5 N for the steel-steel contact to make the Hertzian contact pressure as similar in value as possible for all the material combinations. The maximum Hertzian contact pressure (P_{max}) was calculated as 0.16 GPa in PEEK-steel, 0.10 GPa in PEEK-PEEK and 0.68 GPa in steel-steel, respectively, using an elastic modulus of 3.83 GPa and a Poisson's ratio of 0.33 for PEEK (adapted from a supplier's catalogue). The wear profiles of PEEK plates were measured with a stylus profilometer (SURFCOM 1500 DX2, Tokyo Seimitsu Co., Ltd.).

2.3. Surface Analyses (Nanoindentation, EPMA, Raman)

After-test specimens from PEEK-steel contacts were rinsed with a hydrocarbon solvent and dried before surface analysis. Nanoindentation measurements were performed with an iNano® nanoindenter (NANOMECHANICS, Inc.) equipped with a Berkovich tip. To evaluate the hardness of PEEK as a function of indentation depth, the continuous stiffness measurement (CSM) technique [50–52] was employed by applying a small, sinusoidally varying signal on top of a DC signal driving the indenter. The hardness at each indentation depth was determined by analyzing the response of amplitude and phase. The frequency and displacement amplitude values were 110 Hz and 1 nm, respectively. Under a load range of 50 mN, a target depth of 3 μm and a strain rate of 0.01 s^{-1}, sixteen points at 50 μm intervals were measured inside a wear scar for each PEEK plate. The average hardness at each indentation depth and the standard deviation were then calculated.

Electron Probe Micro Analysis (EPMA) and Raman spectroscopy were carried out on the transfer films found on the steel balls after tribological tests using a JXA-8530F (JEOL Ltd.) and a Renishaw inVia™ Raman spectrometer (Renishaw plc). EPMA is equipped with Wavelength Dispersive X-ray spectroscopy (WDX) which counts the number of X-rays of a specific wavelength diffracted by a crystal, therefore it has higher resolution than Energy Dispersive X-ray spectrometry (EDX) and is suitable for carbon mapping. The secondary electron (SE) images and carbon maps were acquired with a 15-kV beam at 100 nA current. Raman spectroscopy is a useful technique for analyzing polymers as it gives characteristic spectra of their molecular structures based upon the inelastic scattering of photons from the samples. The Raman spectra were obtained between 700 cm^{-1} and 1800 cm^{-1} from 100 scans of 1 second each with a 785 nm laser, using a 20 × objective.

3. Results and Discussion

3.1. OFMs in PEEK-smooth steel contact

The Stribeck curves, representing friction coefficient values as a function of entrainment speed, for the PEEK-smooth

steel contact lubricated with PAO and PAO + OFMs are summarized in **Fig. 4**. While PAO showed slightly higher friction at 200% SRR (sliding) than 50% SRR (sliding-rolling), a significant friction reduction was achieved at both SRRs by the addition of OFM-C (N-oleoyl sarcosine). OFM-A (oleylamine) and OFM-B (oleic acid) also reduced friction, although their impact was much lower than that of OFM-C. The effect of various concentrations of OFM-C (0.01, 0.1 and 1 wt.%) is shown in **Fig. 5**. Interestingly, the remarkable ability of OFM-C to reduce friction efficiently is observable even at the lowest concentration (0.01 wt.%) and has superior results to OFM-A and OFM-B at high concentration (1 wt.%), regardless of SRRs. It is meaningful to mention that when tribological tests were conducted with smooth steel balls, there was almost no wear on the PEEK plates, regardless of SRRs or lubricant formulations.

Theoretically, the different values of SRRs used for testing have no effect on the lubrication regime. In this study the entrainment speeds were the same at 200% SRR (sliding) and 50% SRR (sliding-rolling) and therefore the lubricant film thicknesses and Lambda ratios were similar. Because the testing conditions employed in the PEEK-steel contact were borderline between piezoviscous-elastic and isoviscous-elastic lubrication, the oil film thickness calculations using the equations for piezoviscous-elastic [53] or isoviscous-elastic lubrication [54,55] gave almost the same results. The calculated Lambda ratios of approximately 0.1 to 3 for the PEEK-smooth steel contact in this study indicate that both 200% SRR and 50% SRR tests were performed in the boundary/mixed lubrication regimes.

In the steel-steel contact, OFMs have been reported to reduce friction by adsorbing or reacting on contact surfaces with the polar groups, thus mitigating the direct contact of the two surfaces in mixed and boundary lubrication regimes [38,39]. The friction results of PAO + OFMs imply that the effect of OFMs, especially OFM-C, in the PEEK-smooth steel contact is similar to that in the steel-steel contact, although the adsorption of OFMs on PEEK is uncertain. Further aspects of OFMs ability to adsorb on PEEK and steel surfaces will be investigated in the section 3.2.

As previously mentioned, there are two key factors, i.e. the changes in hardness of PEEK surfaces and the formation of PEEK transfer films on steel counterparts during testing, which influence tribological results of the PEEK-steel contact. The effect of OFMs on the PEEK hardness will be investigated in the section 3.4. The PEEK transfer films proved difficult to detect on smooth steel balls because they were easily removed from smooth surfaces at the end of tests. However, the higher and more unstable friction values for PAO at 200% SRR (**Fig. 4(a)**) imply that the amount of the PEEK transfer film under PAO lubrication was larger at 200% SRR than 50% SRR, therefore the working regime leaned towards boundary lubrication. Additionally, the low and steady friction values achieved with PAO + OFM-C (1%) could indicate that OFM-C influenced the formation of PEEK transfer films on steel. The effect of the OFMs on PEEK transfer films formation will be further discussed in the section 3.5.

3.2. OFMs in PEEK-PEEK and steel-steel contacts

Although this study mainly focused on the PEEK-steel contact, the effect of OFMs in PEEK-PEEK and steel-steel contacts was evaluated to estimate separately the OFM adsorption ability on PEEK and steel surfaces. The Stribeck curves for PEEK-PEEK and steel-steel contacts lubricated with PAO and PAO + OFMs are shown in **Fig. 6**. Similar to the PEEK-smooth steel contact (**Fig. 4**), OFM-C also reduced friction in the PEEK-PEEK and steel-steel contacts at both 200% and 50% SRRs. On the contrary, the friction reducing effects of OFM-A and OFM-B were lower especially at 50% SRR. Different concentrations of OFM-C were also investigated as shown in **Fig. 7**. In both the PEEK-PEEK and steel-steel contacts, OFM-C showed a friction reducing effect even at lower concentrations. These results imply that OFM-C

adsorbed on both PEEK and steel surfaces reducing friction in the PEEK-smooth steel contact as discussed in the former section 3.1.

The poor friction reducing properties of OFM-A and OFM-B in PEEK-PEEK and steel-steel contacts could be due to a low ability to absorb/react on either PEEK and steel surfaces under the test condition i.e. temperature employed in this study. OFM-A (olyelamine) and OFM-B (oleic acid) are widely used organic friction modifiers for many applications, but it has been reported that they generally work better at higher temperatures which accelerate the reaction of their polar groups with the surfaces [43,44]. On the contrary, OFM-C (N-oleoyl sarcosine) achieved a significant friction reduction for both PEEK-PEEK and steel-steel contacts even at very low concentrations. This implies that OFM-C has a superior adsorption ability on both PEEK and steel surfaces at ambient temperature. Sarcosine derivatives of fatty acids have been historically used as a preferred anti-rust additive due to the chelate-forming property of the polar group (**Fig. 8**) which interacts strongly with metal surfaces [56,57]. Chelation may also enhance the adsorption of OFM-C onto PEEK surface which contains the polar ketone groups in the molecule structure [58–60]. It should be noted that OFM-C gave superior friction reduction at 200% SRR than 50% SRR for both PEEK-PEEK and steel-steel contacts. This indicates that the adsorption of OFM-C is greater in 200% SRR (sliding) than 50% SRR (sliding-rolling). As explained in the section 2.2, SRR is defined as the ratio of the sliding speed to the entrainment speed. Therefore, the sliding speeds at each entrainment speed are higher at 200% SRR than 50% SRR, causing higher frictional heat which accelerates the adsorption of OFM-C. This is also supported by the fact that PAO + OFM-C showed lower friction at 200% SRR than 50% SRR for the PEEK-smooth steel contact in the former section 3.1.

3.3. OFMs in PEEK-rough steel contact

To investigate the effect of OFMs in the PEEK-steel contact under more severe boundary lubrication, tribological tests were performed with rough steel balls and Lambda ratios between 0.01-0.3. The Stribeck curves lubricated with PAO and PAO + OFMs are shown in **Fig. 9**. Under PAO lubrication, the friction was considerably higher at 50% SRR than at 200% SRR. With the addition of OFMs an opposite effect on friction was recorded depending on the SRR. At 200% SRR (sliding) OFMs reduced friction when added to PAO. By contrast, at 50% SRR (sliding-rolling) OFMs, especially OFM-C, increased friction. This friction increasing effect of OFM-C at 50% SRR was more significant at entrainment speeds above 0.1 m/s. The effect of different concentrations of OFM-C was also investigated (**Fig. 10**) and while at 200% SRR no difference in friction was observed, at 50% SRR the two higher concentrations (0.1 and 1 wt.%) increased friction.

The optical images and wear profiles of after-test PEEK plates in **Fig. 11** show a very good correlation between the wear and friction results i.e. higher friction led to increased wear for all lubricants. The wear volumes of PEEK plates lubricated with PAO were higher at 50% SRR than at 200% SRR (**Fig. 11(e, m)**). The OFM-A and OFM-B did not affect wear while OFM-C showed significantly reduced wear at 200% SRR and increased it at 50% SRR (**Fig. 11(h, p)**). At 200% SRR (sliding) OFM-C preserved the smoothness of the wear tracks even in the lower concentrations (**Fig. 11(u, v)**). On the contrary, at 50% SRR (sliding-rolling) OFM-C increased the wear volumes of PEEK plates even in the lower concentrations (**Fig. 11(w, x)**).

Thus, in the PEEK-smooth steel contact OFM-C reduced friction at both 50% and 200% SRRs as discussed in the section 3.1, while in the PEEK-rough steel contact OFM-C affected friction and wear in opposite ways depending on SRR. Considering that the calculated Lambda ratios at both SRRs were theoretically the same, the significant difference

between the friction and wear behavior at 200% and 50% SRRs in the PEEK-rough steel contact may depend on the two key factors: the changes in hardness of PEEK surfaces and the formation of PEEK transfer films on the steel counterparts. Therefore, these factors were carefully investigated in the following sections 3.4 and 3.5.

3.4. Hardness modification of PEEK surfaces

The nanoindentation measurements were carried out on the wear scars of PEEK plates from PEEK-steel tests lubricated with PAO and PAO + OFM-C (1%) because OFM-C showed the most significant impact on friction and wear. The hardness values were plotted as a function of indentation depth and compared to those of a new PEEK plate (**Fig. 12**). In all tests, hardness showed high values at indentation depth <0.5 μm. These values are thought to be attributed to a phenomenon known as indentation size effect (ISE), and are not regarded as physically significant because they are distorted by the inadequacies in the procedures applied to provide corrections for the imperfections in the tip geometry [52,61]. Therefore, PEEK hardness measurements at indentation depth larger than 0.5 μm were used.

The nanoindentation measurement results indicate that there was no correlation between the hardness of PEEK surfaces and the friction and wear properties. In the case of PEEK-smooth steel contact, the hardness of PEEK plate tested with PAO was lower at 200% SRR than at 50% SRR (**Fig. 12(a, c)**), while friction was higher at 200% SRR than at 50% SRR (**Fig. 4**). On the other hand, PAO + OFM-C (1%) also led to lower PEEK hardness at 200% SRR than at 50% SRR (**Fig. 12(b, d)**), but showed lower friction at 200% SRR than at 50% SRR (**Fig. 4**). A similar discrepancy was also observed in the PEEK-rough steel case. At both SRRs, the values of PEEK hardness when lubricated with PAO + OFM-C (1%) (**Fig. 12(f, h)**) were higher than when lubricated with PAO (**Fig. 12(e, g)**). Although, OFM-C affected friction and wear properties in opposite ways depending on SRRs, i.e. improving friction and wear at 200% SRR (**Fig. 9(a), Fig. 11(h)**) or worsening them at 50% SRR (**Fig. 9(b), Fig. 11(p)**).

Further investigations are required to understand the detailed mechanism of hardness modification of PEEK surfaces under lubricated contacts. The results discussed above suggest that the hardness of PEEK surfaces does not greatly affect the tribological performance in this study and that other factors could have a more important role. Therefore, the other key factor, formation of PEEK transfer films on steel counterparts was investigated in the following section 3.5.

3.5. PEEK transfer films on steel balls

The PEEK transfer films were investigated on the rough steel balls because they were entrapped between asperities of steel surfaces and more consistent than those on the smooth steel balls. In addition, the study focused on the specimens tested with PAO and PAO + OFM-C (1%) as for nanoindentation measurements. Secondary Electron (SE) images of all specimens in **Fig. 13(a-d)** showed that there was almost no wear on steel balls. As the hardness of a steel ball is much higher than that of a PEEK plate, it was expected that wear would mainly occur on PEEK plates. Notably the shapes of wear scars were different between 200% SRR (sliding) and 50% SRR (sliding-rolling) tests. In sliding tests (200% SRR) the steel balls were fixed and the wear scars had a round shape (**Fig. 13(a, b)**), while in sliding-rolling tests (50% SRR) the steel balls rotated producing a circumferential wear scar (**Fig. 13(c, d)**). Although SE images clearly indicate the presence of PEEK transfer films, to evaluate the PEEK amount, EPMA carbon mapping was also employed **Fig. 13(e-h)**. The carbon amount is indicated by the color scale on the map. On the wear scars of the steel balls lubricated with PAO, larger amounts of carbon were detected at 200% SRR than at 50% SRR (**Fig. 13(e, g)**). By adding OFM-C, the carbon

amount was reduced at both SRRs (**Fig. 13(f, h)**), and this reduction was observed not only inside wear scars but also outside.

The presence of carbon detected with EPMA is supposedly related to PEEK transfer films but to confirm this assumption Raman spectra were recorded on the wear scars of steel balls as shown in **Fig. 13(i-l)**. All spectra display identical peaks which match the Raman spectra of PEEK reported in the literature [62–65]. A small difference is observed around 1300 cm^{-1} in the spectra for PAO and PAO + OFM-C (1%) at 50% SRR (**Fig. 13(k, l)**) which could be caused by the steel substrate. From the Raman spectroscopy results, it can be concluded that EPMA carbon mapping is a valid analysis technique for PEEK transfer films on steel balls.

It is noteworthy that the carbon amount on the wear scars of steel balls (**Fig. 13(e-h)**) and the friction and wear properties (**Fig. 9 and Fig. 11**) showed a good correlation i.e. in the PEEK-rough steel contact a greater amount of carbon on the steel counterparts led to lower friction and wear. This indicates that the presence of a PEEK transfer film on the steel ball is a key factor in controlling tribological performances of the PEEK-rough steel contact. As discussed in the section 3.3, OFM-C had a detrimental effect on friction and wear at 50% SRR (**Fig. 9(b), Fig. 11(p)**). The lower carbon amount on the steel ball lubricated with PAO + OFM-C (1%) at 50% SRR (**Fig. 13(h)**) suggests that the PEEK transfer film was not thick enough to cover the roughness of the steel ball. This caused abrasive wear by direct contact between the PEEK surface and the large asperities of the steel surfaces. In this case the adsorption of OFM-C on the steel surface may have inhibited the formation of a thick PEEK transfer film. As we reported previously [31], PAO lubrication by itself inhibits the formation of transfer films compared to dry conditions. In this study, the adsorption of OFMs was found to inhibit even more the formation of PEEK transfer films. In steel-steel contacts, similar competitions between OFMs and anti-wear ZDDP or phosphorous agents to absorb/react on the wear track have been reported by Ratoi et al. [66] and Onumata et al. [67]. As already mentioned, the carbon amounts outside wear scars were very limited for PAO + OFM-C (1%) regardless of SRRs (**Fig. 13(f, h)**). This implies that OFM-C adsorbed not only inside but also outside the wear scars on steel balls and thus inhibited the formation of PEEK transfer films.

Intriguing, the thick transfer film was formed at 200% SRR even in the PAO + OFM-C (1%) lubricated test (**Fig. 13(f)**). This implies that in sliding (200% SRR) conditions the PEEK film transfer was more dominant than the inhibition by OFM-C adsorption and thus it controlled the process. Puhan and Wong [64] reported in-situ observation of the PEEK wear process under dry conditions and suggested that PEEK wear debris ploughed by the asperities of the counter surface re-entered the contact surfaces, forming PEEK transfer films. Under lubricated conditions, wear debris particles once formed disperse into the lubricant. However, the sliding (200% SRR) in which the steel ball is fixed, can help to trap and pile up formed wear debris near the contact inlet more efficiently than the sliding-rolling (50% SRR) where both the steel ball and the PEEK plate rotate and aid the flushing out wear debris. The accumulated wear debris near the inlet can contribute to the formation of a PEEK transfer film on the steel surface in sliding (200% SRR) even under lubrication with PAO + OFM-C (1%) (**Fig. 13(f)**). In addition, PAO + OFM-C (1%) showed lower friction and wear (the surface profile with almost no wear) than PAO at 200% SRR (**Fig. 9(a), Fig. 11(h)**). This implies that OFM-C adsorbed on both the PEEK plate and the PEEK transfer film on the steel ball, thus mitigating the severity of the contact conditions between the two surfaces.

As discussed in the section 3.1, the advanced film transfer in the PEEK-smooth steel contact lubricated with PAO at 200% SRR increased friction. Contrary to the PEEK-rough steel contact, the PEEK transfer films in this case exerted a negative effect on friction by increasing the surface roughness and shifting the lubrication regime closer to the boundary

lubrication. The outstanding friction reduction property showed by PAO + OFM-C (1%) at 200% SRR (**Fig. 4(a)**) can be achieved by the synergistic effect of OFM adsorption and the inhibition of excessive PEEK transfer films on steel counterparts.

3.6. Mechanism of lubrication

Although OFM-C affected the hardness of PEEK surfaces as shown in the section 3.4, no correlation was found between the PEEK hardness and tribological performances of the PEEK-steel contact. In this study, it is assumed that the friction and wear of PEEK-steel contact under lubrication with OFM added to PAO is mainly controlled by the OFM adsorption and the PEEK transfer film. Considering these factors, the proposed mechanism of lubrication with OFMs in the PEEK-steel contact is summarized in **Fig. 14**. The working mechanism has been investigated by focusing on OFM-C in the sections 3.4 and 3.5 but it has been generalized for OFMs, because most OFMs can be considered to work at ambient temperature essentially in the same way as OFM-C although the extent depends on their adsorption abilities.

OFMs adsorb on both steel and PEEK surfaces with the polar group. The lubrication mechanism in the PEEK-smooth steel contact is similar to that of steel-steel contact: the OFM adsorption layer mitigates the direct contact between the two surfaces and thus reduces friction. Furthermore, the OFMs adsorption on the smooth steel surface inhibits the formation of excessive PEEK transfer films which would increase friction by increasing surface roughness. The adsorption of OFMs is greater in sliding than sliding-rolling, resulting in superior friction reduction. For the PEEK-smooth steel contact OFMs show positive effects in both sliding and sliding-rolling. By contrast, for the PEEK-rough steel contact, OFMs show either a positive or negative effect on friction and wear depending on the type of contact motion. In sliding, a thick and stable PEEK transfer film is formed on the rough steel surface even under lubrication with PAO + OFMs. OFMs adsorb on top of the PEEK transfer film and on the PEEK plate surface, reducing friction and wear. However, this scenario changes in sliding-rolling where OFM adsorption on rough steel inhibits the formation of PEEK transfer film, and thus preserving the steel ball roughness. As a result, abrasive wear between the asperities of the steel surface and the PEEK plate causes increased friction and wear of PEEK.

Both OFM adsorption and PEEK transfer on steel counterparts are affected by the tribological conditions. Thus, in practical applications the balance between these two processes depends on the specific conditions used. Having said that, this study brings novel insight into the effect of OFMs on lubrication of PEEK-steel contact by elucidating the working mechanism of OFMs which is essential to formulating optimal lubricants and developing more efficient systems for PEEK applications.

4. Conclusions

The effect of OFMs on lubrication of PEEK-steel contacts has been investigated by varying the types of contact motion, the material pairing and the roughness of steel surfaces. The results were corroborated and analyzed by focusing on two key factors, the hardness of PEEK surfaces and the PEEK transfer films, and a working mechanism of OFMs has been defined. The following conclusions have been drawn:

(1) Compared with OFM-A (oleylamine) and OFM-B (oleic acid), OFM-C (N-oleoyl sarcosine) showed a significant friction reduction in the PEEK-smooth steel contact at both 200% SRR (sliding) and 50% SRR (sliding-rolling).

A similar friction reducing effect of OFM-C was seen in the PEEK-PEEK and steel-steel contacts;

(2) In the PEEK-rough steel contact OFMs, most significantly OFM-C, showed opposite effects depending on SRRs, reducing friction and wear at 200% SRR while increasing them at 50% SRR;

(3) The hardness of PEEK surfaces was affected by the addition of OFM-C, but no correlation was observed between the PEEK hardness and the tribological properties of the PEEK-steel contact;

(4) A good correlation was observed between the amount of PEEK transfer films and the tribological properties of the PEEK-steel contact. OFM-C inhibited the formation of PEEK transfer films, which can have either a positive or negative effect on tribological properties depending on the test conditions.

This study elucidated the effect of OFMs on lubrication of the PEEK-steel contact and proposed the mechanism of action. This knowledge contributes to designing efficient tribological systems and formulating suitable lubricants for PEEK-steel applications and thus promoting the rapid adoption of green technologies in many applications.

Acknowledgements

The authors would like to thank Mr. Shinji Hasegawa from JXTG Nippon Oil & Energy Corporation for performing the nanoindentation measurements and the Analytical Technology group from R&D Solution Center, JXTG Nippon Oil & Energy Corporation for performing EPMA. This work was sponsored by JXTG Nippon Oil & Energy Corporation.

References

[1] Myshkin NK, Pesetskii SS, Grigoriev AY. Polymer tribology: current state and applications. Tribol Ind 2015;37:284–90.

[2] Gandhi R, Jayawant A, Bhalerao A, Dandagwhal R. Applicability of composite polymer gear in low RPM applications – a review. Int J Eng Sci Invent 2018;7:36–41.

[3] Friedrich K. Polymer composites for tribological applications. Adv Ind Eng Polym Res 2018;1:3–39. doi:10.1016/j.aiepr.2018.05.001.

[4] Kurdi A, Chang L. Recent advances in high performance polymers – tribological aspects. Lubricants 2018;7:2–10. doi:10.3390/lubricants7010002.

[5] Nunez EE, Gheisari R, Polycarpou AA. Tribology review of blended bulk polymers and their coatings for high-load bearing applications. Tribol Int 2019;129:92–111. doi:10.1016/j.triboint.2018.08.002.

[6] Walton D, Shi YW. A comparison of ratings for plastic gears. Proc Inst Mech Eng Part C J Mech Eng Sci 1989;203:31–8. doi:10.1243/PIME_PROC_1989_203_083_02.

[7] Hooke CJ, Kukureka SN, Liao P, Rao M, Chen YK. The friction and wear of polymers in non-conformal contacts. Wear 1996;200:83–94. doi:10.1016/S0043-1648(96)07270-5.

[8] Briscoe BJ, Sinha SK. Wear of polymers. Proc Inst Mech Eng Part J J Eng Tribol 2002;216:401–13. doi:10.1243/135065002762355325.

[9] Singh AK, Siddhartha, Singh PK. Polymer spur gears behaviors under different loading conditions: a review. Proc Inst Mech Eng Part J J Eng Tribol 2018;232:210–28. doi:10.1177/1350650117711595.

[10] Harrass M, Friedrich K, Almajid AA. Tribological behavior of selected engineering polymers under rolling contact. Tribol Int 2010;43:635–46. doi:10.1016/j.triboint.2009.10.003.

[11] Kurdi A, Kan WH, Chang L. Tribological behaviour of high performance polymers and polymer composites at elevated temperature. Tribol Int 2019;130:94–105. doi:10.1016/j.triboint.2018.09.010.

[12] Schelling A, Kausch HH, Roulin AC. Friction behaviour of polyetheretherketone under dry reciprocating movement. Wear 1991;151:129–42. doi:10.1016/0043-1648(91)90353-V.

[13] Lu ZP, Friedrich K. On sliding friction and wear of PEEK and its composites. Wear 1995;181–183:624–31. doi:10.1016/0043-1648(95)90178-7.

[14] Laux KA, Schwartz CJ. Influence of linear reciprocating and multi-directional sliding on PEEK wear performance and transfer film formation. Wear 2013;301:727–34. doi:10.1016/j.wear.2012.12.004.

[15] Hoskins TJ, Dearn KD, Chen YK, Kukureka SN. The wear of PEEK in rolling-sliding contact - simulation of polymer gear applications. Wear 2014;309:35–42. doi:10.1016/j.wear.2013.09.014.

[16] Laux KA, Jean-Fulcrand A, Sue HJ, Bremner T, Wong JSS. The influence of surface properties on sliding contact temperature and friction for polyetheretherketone (PEEK). Polymer (Guildf) 2016;103:397–404. doi:10.1016/j.polymer.2016.09.064.

[17] Zalaznik M, Kalin M, Novak S. Influence of the processing temperature on the tribological and mechanical properties of poly-ether-ether-ketone (PEEK) polymer. Tribol Int 2016;94:92–7. doi:10.1016/j.triboint.2015.08.016.

[18] Lin L, Pei XQ, Bennewitz R, Schlarb AK. Friction and wear of PEEK in continuous sliding and unidirectional scratch tests. Tribol Int 2018;122:108–13. doi:10.1016/j.triboint.2018.02.035.

[19] Yahiaoui M, Chabert F, Paris JY, Nassiet V, Denape J. Friction, acoustic emission, and wear mechanisms of a PEKK polymer. Tribol Int 2019;132:154–64. doi:10.1016/j.triboint.2018.12.020.

[20] Qihua W, Jinfen X, Weichang S, Weimin L. An investigation of the friction and wear properties of nanometer Si3N4 filled PEEK. Wear 1996;196:82–6.

[21] Minami I, Kubo T, Nanao H, Mori S, Iwata H, Fujita M. Surface chemistry for improvement in load-carrying capacity of poly(ether-ether-ketone)-based materials by poly(tetrafluoroethylene). Tribol Online 2008;3:190–4. doi:10.2474/trol.3.190.

[22] Greco AC, Erck R, Ajayi O, Fenske G. Effect of reinforcement morphology on high-speed sliding friction and wear of PEEK polymers. Wear 2011;271:2222–9. doi:10.1016/j.wear.2011.01.065.

[23] Kalin M, Zalaznik M, Novak S. Wear and friction behaviour of poly-ether-ether-ketone (PEEK) filled with graphene, WS2 and CNT nanoparticles. Wear 2015;332–333:855–62. doi:10.1016/j.wear.2014.12.036.

[24] Rodriguez V, Sukumaran J, Schlarb AK, De Baets P. Influence of solid lubricants on tribological properties of polyetheretherketone (PEEK). Tribol Int 2016;103:45–57. doi:10.1016/j.triboint.2016.06.037.

[25] Theiler G, Gradt T. Environmental effects on the sliding behaviour of PEEK composites. Wear 2016;368–369:278–86. doi:10.1016/j.wear.2016.09.019.

[26] Lin L, Schlarb AK. Tribological response of the PEEK/SCF/graphite composite by releasing rigid particles into the tribosystem. Tribol Int 2019;137:173–9. doi:10.1016/j.triboint.2019.05.002.

[27] Sumer M, Unal H, Mimaroglu A. Evaluation of tribological behaviour of PEEK and glass fibre reinforced PEEK composite under dry sliding and water lubricated conditions. Wear 2008;265:1061–5. doi:10.1016/j.wear.2008.02.008.

[28] Chen B, Wang J, Yan F. Comparative investigation on the tribological behaviors of CF/PEEK composites under sea water lubrication. Tribol Int 2012;52:170–7. doi:10.1016/j.triboint.2012.03.017.

[29] Minn M, Sinha SK. The lubrication of poly(etheretherketone) by an aqueous solution of nattokinase. Wear 2012;296:528–35. doi:10.1016/j.wear.2012.08.008.

[30] Zhang G, Wetzel B, Wang Q. Tribological behavior of PEEK-based materials under mixed and boundary lubrication conditions. Tribol Int 2015;88:153–61. doi:10.1016/j.triboint.2015.03.021.

[31] Tatsumi G, Ratoi M, Shitara Y, Sakamoto K, Mellor BG. Effect of lubrication on friction and wear properties of PEEK with steel counterparts. Tribol Online 2019;14:345–52. doi:10.2474/trol.14.345.

[32] de Andrade TF, Wiebeck H, Sinatora A. Tribology of natural poly-ether-ether-ketone (PEEK) under transmission oil lubrication. Polimeros 2019;29:3–11. doi:10.1590/0104-1428.14416.

[33] Wu C, Wei C, Jin X, Akhtar R, Zhang W. Carbon spheres as lubricant additives for improving tribological performance of polyetheretherketone. J Mater Sci 2019;54:5127–35. doi:10.1007/s10853-018-3177-4.

[34] Yu G, Liu H, Mao K, Zhu C, Wei P, Lu Z. An experimental investigation on the wear of lubricated steel against PEEK gears. J Tribol 2020;142:1–7. doi:10.1115/1.4045627.

[35] Miller A. The chemistry of lubricating oil additives. J Chem Educ 2009;33:308. doi:10.1021/ed033p308.

[36] Minami I. Molecular science of lubricant additives. Appl Sci 2017;7:445–77. doi:10.3390/app7050445.

[37] Sniderman D. The chemistry and function of lubricant additives. Tribol Lubr Technol 2017;73:18–28.

[38] Tang Z, Li S. A review of recent developments of friction modifiers for liquid lubricants (2007-present). Curr Opin Solid State Mater Sci 2014;18:119–39. doi:10.1016/j.cossms.2014.02.002.

[39] Spikes H. Friction modifier additives. Tribol Lett 2015;60:1–26. doi:10.1007/s11249-015-0589-z.

[40] Ratoi M, Anghel V, Bovington C, Spikes HA. Mechanisms of oiliness additives. Tribol Int 2000;33:241–7. doi:10.1016/S0301-679X(00)00037-2.

[41] Ratoi M, Bovington C, Spikes H. In situ study of metal oleate friction modifier additives. Tribol Lett 2003;14:33–40. doi:10.1023/A:1021714231949.

[42] Hirayama T, Torii T, Konishi Y, Maeda M, Matsuoka T, Inoue K, et al. Thickness and density of adsorbed additive layer on metal surface in lubricant by neutron reflectometry. Tribol Int 2012;54:100–5. doi:10.1016/j.triboint.2012.04.012.

[43] Simič R, Kalin M. Adsorption mechanisms for fatty acids on DLC and steel studied by AFM and tribological experiments. Appl Surf Sci 2013;283:460–70. doi:10.1016/j.apsusc.2013.06.131.

[44] Loehle S, Matta C, Minfray C, Mogne T Le, Martin JM, Iovine R, et al. Mixed lubrication with C18 fatty acids: effect of unsaturation. Tribol Lett 2014;53:319–28. doi:10.1007/s11249-013-0270-3.

[45] Yamamoto Y, Hashimoto M. Friction and wear of water lubricated PEEK and PPS sliding contacts. Wear 2002;253:820–6. doi:10.1016/j.wear.2003.12.004.

[46] Yamaguchi T, Hokkirigawa K. Friction and wear properties of peek resin filled with RB ceramics particles under water lubricated condition. Tribol O 2016;11:653–60. doi:10.2474/trol.11.653.

[47] Briscoe BJ, Stolarski TA, Davies GJ. Boundary lubrication of thermoplastic polymers in model fluids. Tribol Int 1984;17:129–37. doi:10.1016/0301-679X(84)90002-1.

[48] Bahadur S. The development of transfer layers and their role in polymer tribology. Wear 2000;245:92–9. doi:10.1016/S0043-1648(00)00469-5.

[49] Kurdi A, Wang H, Chang L. Effect of nano-sized TiO2 addition on tribological behaviour of poly ether ether ketone composite. Tribol Int 2018;117:225–35. doi:10.1016/j.triboint.2017.09.002.

[50] Li X, Bhushan B. A review of nanoindentation continuous stiffness measurement technique and its applications. Mater Charact 2002;48:11–36. doi:10.1016/S1044-5803(02)00192-4.

[51] Iqbal T, Briscoe BJ, Luckham PF. Surface plasticization of poly(ether ether ketone). Eur Polym J 2011;47:2244–58. doi:10.1016/j.eurpolymj.2011.09.022.

[52] Voyiadjis GZ, Samadi-Dooki A, Malekmotiei L. Nanoindentation of high performance semicrystalline polymers: a case study on PEEK. Polym Test 2017;61:57–64. doi:10.1016/j.polymertesting.2017.05.005.

[53] Hamrock BJ, Dowson D. Isothermal elastohydrodynamic lubrication of point contacts III - fully flooded results. NASA Tech Note 1976;D-8317. doi:10.1016/s0165-0270(01)00342-9.

[54] Hamrock BJ, Dowson D. Elastohydrodynamic lubrication of elliptical contacts for materials of low elastic modulus. 1-Fully flooded conjunction. NASA Tech Note 1977;D-8528.

[55] Marx N, Guegan J, Spikes HA. Elastohydrodynamic film thickness of soft EHL contacts using optical interferometry. Tribol Int 2016;99:267–77. doi:10.1016/j.triboint.2016.03.020.

[56] Salensky GA, Cobb MG, Everhart DS. Corrosion-inhibitor orientation on steel. Ind Eng Chem Prod Res Dev 1986;25:133–40. doi:10.1021/i300022a002.

[57] Kaskah SE, Pfeiffer M, Klock H, Bergen H, Ehrenhaft G, Ferreira P, et al. Surface protection of low carbon steel with N-acyl sarcosine derivatives as green corrosion inhibitors. Surfaces and Interfaces 2017;9:70–8. doi:10.1016/j.surfin.2017.08.002.

[58] Chen HL, You JW, Porter RS. Intermolecular interaction and conformation in poly(ether ether ketone)/poly(ether imide) blends - an infrared spectroscopic investigation. J Polym Res 1996;3:151–8. doi:10.1007/BF01494524.

[59] Roy S, Sahoo NG, Kuo H, Cheng F, Das CK, Chan SH, et al. Molecular interaction and properties of poly(ether ether ketone)/liquid crystalline polymer blends incorporated with functionalized carbon nanotubes. J Nanosci Nanotechnol 2011;11:10408–16. doi:10.1166/jnn.2011.5110.

[60] Li D, Shi D, Feng K, Li X, Zhang H. Poly(ether ether ketone) (PEEK) porous membranes with super high thermal stability and high rate capability for lithium-ion batteries. J Memb Sci 2017;530:125–31. doi:10.1016/j.memsci.2017.02.027.

[61] Bonne M, Briscoe BJ, Lawrence CJ, Manimaaran S, Parsonage D, Allan A. Nano-indentation of scratched poly(methyl methacrylate) surfaces. Tribol Lett 2005;18:125–33. doi:10.1007/s11249-004-1767-6.

[62] Ellis G, Naffakh M, Marco C, Hendra PJ. Fourier transform Raman spectroscopy in the study of technological polymers part 1: poly(aryl ether ketones), their composites and blends. Spectrochim Acta - Part A Mol Biomol Spectrosc 1997;53:2279–94. doi:10.1016/S1386-1425(97)00168-6.

[63] Stuart BH. Application of Raman spectroscopy to the tribology of polymers. Tribol Int 1998;31:687–93. doi:10.1016/S0301-679X(98)00089-9.

[64] Puhan D, Wong JSS. Properties of polyetheretherketone (PEEK) transferred materials in a PEEK-steel contact. Tribol Int 2019;135:189–99. doi:10.1016/j.triboint.2019.02.028.

[65] Doumeng M, Ferry F, Delbé K, Mérian T, Chabert F, Berthet F, et al. Evolution of crystallinity of PEEK and

glass-fibre reinforced PEEK under tribological conditions using Raman spectroscopy. Wear 2019;426–427:1040–6. doi:10.1016/j.wear.2018.12.078.

[66] Ratoi M, Niste VB, Alghawel H, Suen YF, Nelson K. The impact of organic friction modifiers on engine oil tribofilms. RSC Adv 2014;4:4278–85. doi:10.1039/c3ra46403b.

[67] Onumata Y, Zhao H, Wang C, Morina A, Neville A. Interactive effect between organic friction modifiers and additives on friction at metal pushing V-belt CVT components. Tribol Trans 2018;61:474–81. doi:10.1080/10402004.2017.1355502.

Tables

Table 1 Test oil formulations

Lubricant	Composition
PAO + OFM-A (1%)	PAO + 1 wt.% Oleylamine
PAO + OFM-B (1%)	PAO + 1 wt.% Oleic acid
PAO + OFM-C (1%)	PAO + 1 wt.% N-oleoyl sarcosine
PAO + OFM-C (0.1%)	PAO + 0.1 wt.% N-oleoyl sarcosine
PAO + OFM-C (0.01%)	PAO + 0.01 wt.% N-oleoyl sarcosine

Figure captions

Fig. 1. Chemical structures of OFMs.

Fig. 2. MTM (a) set-up appearance and schematic configurations of (b) PEEK-steel, (c) PEEK-PEEK and (d) steel-steel.

Fig. 3. Friction coefficient and entrainment speed as a function of time during the tribological test.

Fig. 4. Stribeck curves for PEEK-smooth steel contact lubricated with PAO and PAO + OFMs at (a) 200% SRR and (b) 50% SRR.

Fig. 5. Stribeck curves for PEEK-smooth steel contact lubricated with PAO and PAO + OFM-C at (a) 200% SRR and (b) 50% SRR.

Fig. 6. Stribeck curves lubricated with PAO and PAO + OFMs for (a) PEEK-PEEK contact at 200% SRR, (b) PEEK-PEEK contact at 50% SRR, (c) steel-steel contact at 200% SRR and (d) steel-steel contact at 50% SRR.

Fig. 7. Stribeck curves lubricated with PAO and PAO + OFM-C for (a) PEEK-PEEK contact at 200% SRR, (b) PEEK-PEEK contact at 50% SRR, (c) steel-steel contact at 200% SRR and (d) steel-steel contact at 50% SRR.

Fig. 8. Schematic effect of a sarcosine derivative of fatty acids on a metal surface.

Fig. 9. Stribeck curves for PEEK-rough steel contact lubricated with PAO and PAO + OFMs at (a) 200% SRR and (b) 50% SRR.

Fig. 10. Stribeck curves for PEEK-rough steel contact lubricated with PAO and PAO + OFM-C at (a) 200% SRR and (b) 50% SRR.

Fig. 11. PEEK plates (a-d, i-l, q-t) optical images and (e-h, m-p, u-x) wear profiles with rough steel balls. Arrows indicate the sliding direction.

Fig. 12. Nanoindentation hardness of PEEK plates tested with (a-d) smooth and (e-h) rough steel balls.

Fig. 13. Wear scars on rough steel balls (a-d) SE images, (e-h) EMPA carbon maps and (i-l) Raman spectra. Arrows indicate the sliding direction.

Fig. 14. Proposed mechanism of lubrication with OFM in PEEK-steel contact.

Fig. 1.

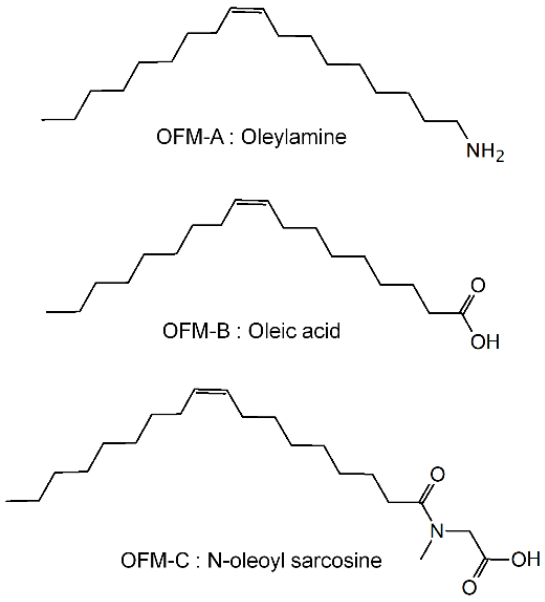
OFM-A : Oleylamine
NH2
OFM-B : Oleic acid
O
OH
OFM-C : N-oleoyl sarcosine
O
N
OH
O

Fig. 2.

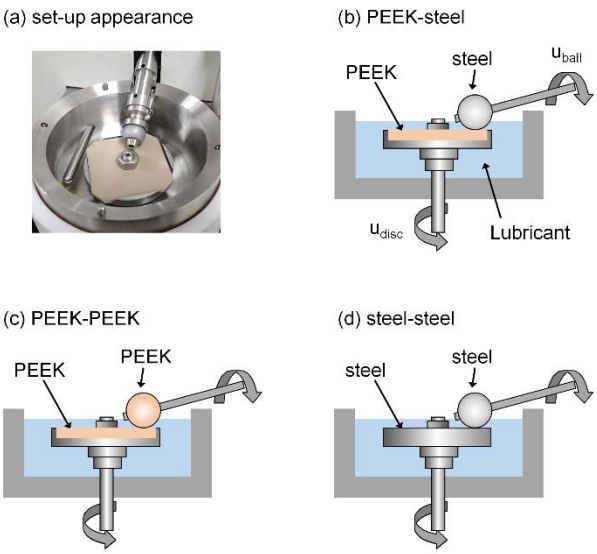
(a) set-up appearance
(b) PEEK-steel
PEEK
steel
u_ball
u_disc
Lubricant
(c) PEEK-PEEK
PEEK
PEEK
(d) steel-steel
steel
steel

Fig. 3.

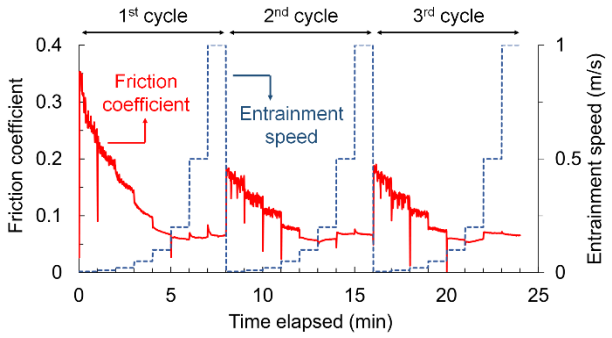

Fig. 4.

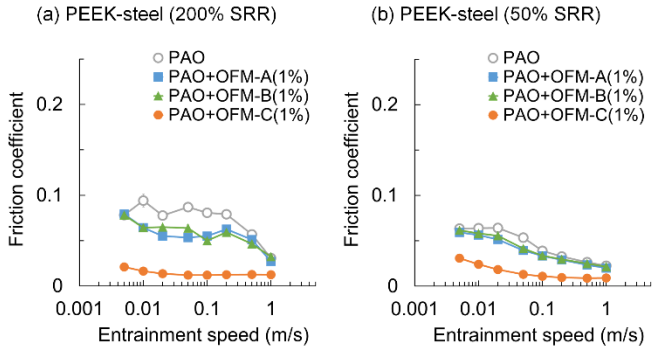

Fig. 5.

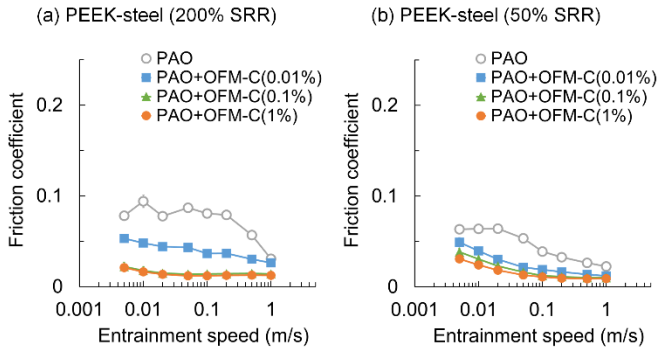

Fig. 6.

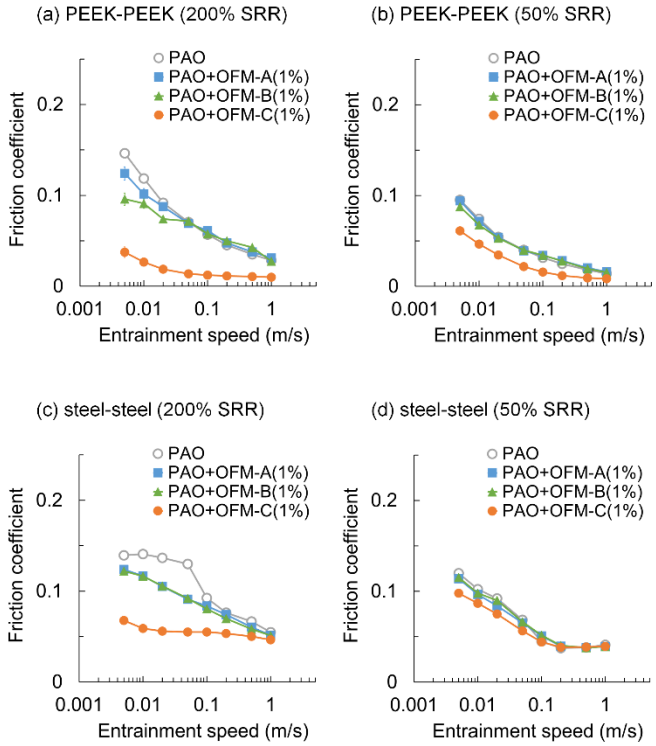
(a) PEEK-PEEK (200% SRR)
(b) PEEK-PEEK (50% SRR)
(c) steel-steel (200% SRR)
(d) steel-steel (50% SRR)
PAO
PAO+OFM-A(1%)
PAO+OFM-B(1%)
PAO+OFM-C(1%)
Friction coefficient
0
0.1
0.2
0.001
0.01
0.1
1
Entrainment speed (m/s)

Fig. 7.

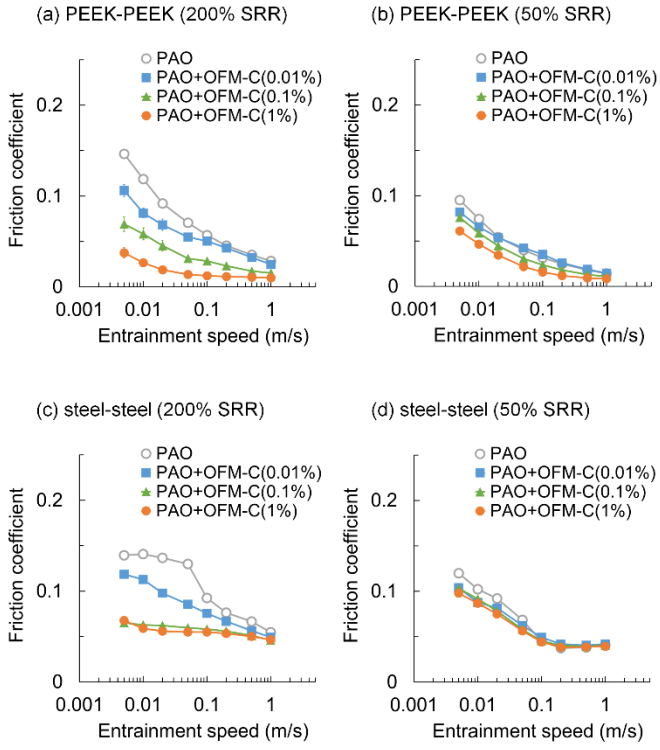
(a) PEEK-PEEK (200% SRR)
(b) PEEK-PEEK (50% SRR)
(c) steel-steel (200% SRR)
(d) steel-steel (50% SRR)
PAO
PAO+OFM-C(0.01%)
PAO+OFM-C(0.1%)
PAO+OFM-C(1%)
Friction coefficient
0
0.1
0.2
0.001
0.01
0.1
1
Entrainment speed (m/s)

Fig. 8.

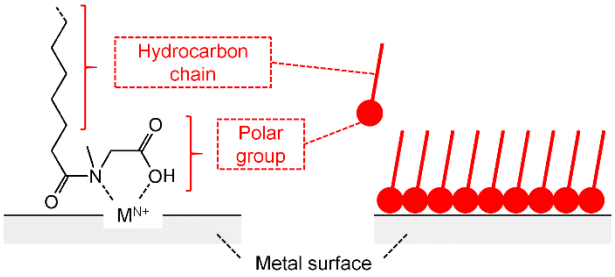

Fig. 9.

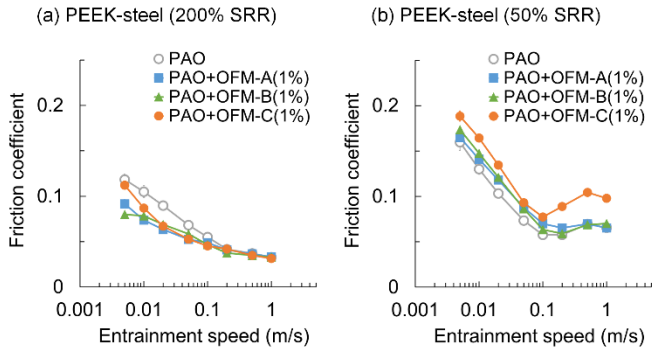

Fig. 10.

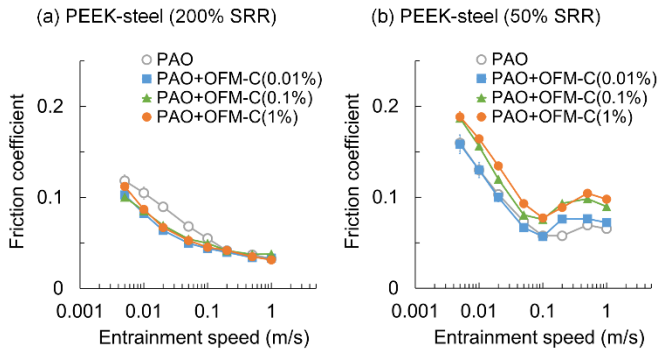

Fig. 11.

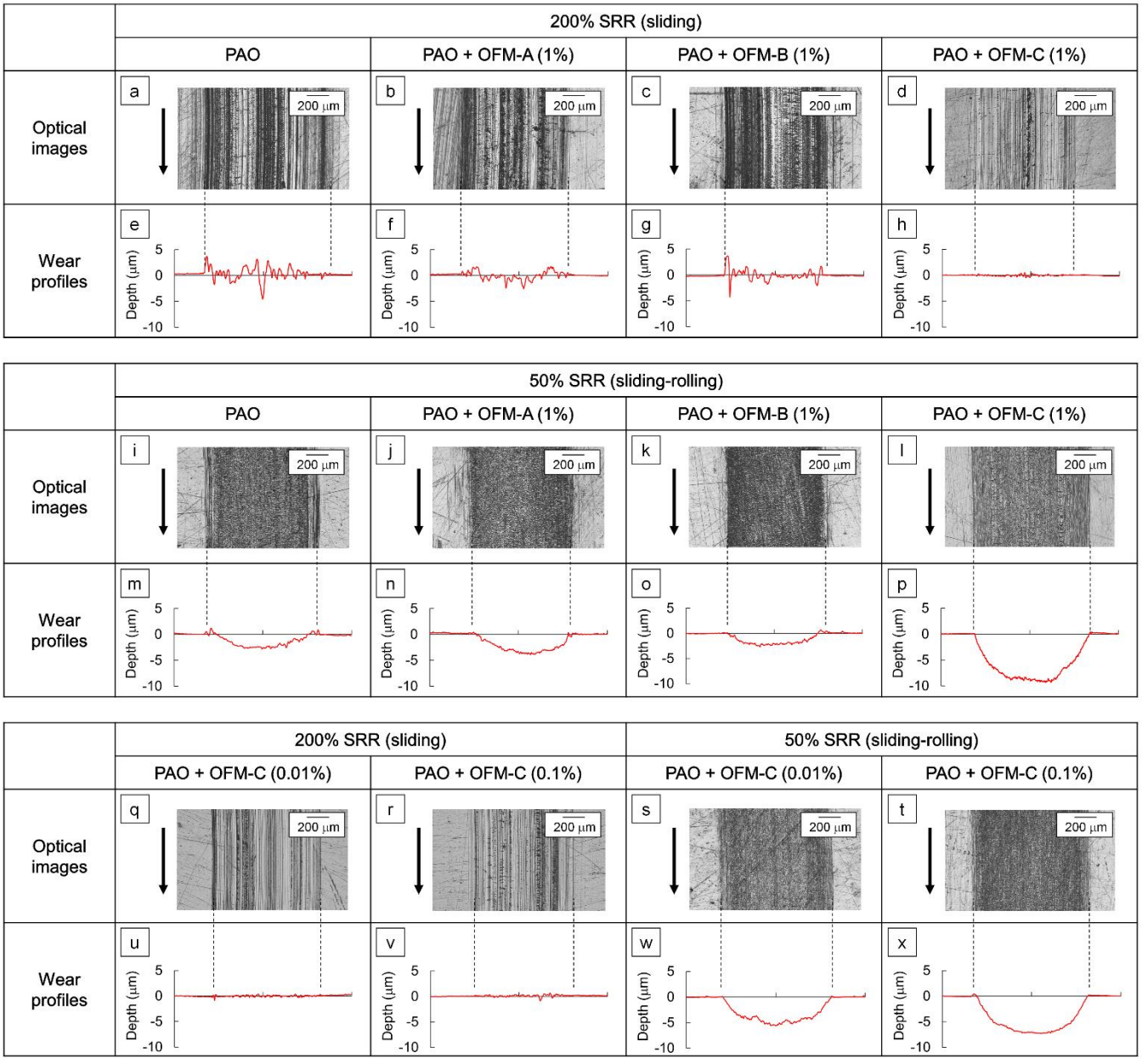
200% SRR (sliding)
PAO
PAO + OFM-A (1%)
PAO + OFM-B (1%)
PAO + OFM-C (1%)
Optical images
Wear profiles
a
b
c
d
e
f
g
h
200 µm
Depth (µm)
5
0
-5
-10
50% SRR (sliding-rolling)
PAO
PAO + OFM-A (1%)
PAO + OFM-B (1%)
PAO + OFM-C (1%)
Optical images
Wear profiles
i
j
k
l
m
n
o
p
200 µm
Depth (µm)
5
0
-5
-10
200% SRR (sliding)
50% SRR (sliding-rolling)
PAO + OFM-C (0.01%)
PAO + OFM-C (0.1%)
PAO + OFM-C (0.01%)
PAO + OFM-C (0.1%)
Optical images
Wear profiles
q
r
s
t
u
v
w
x
200 µm
Depth (µm)
5
0
-5
-10

Fig. 12.

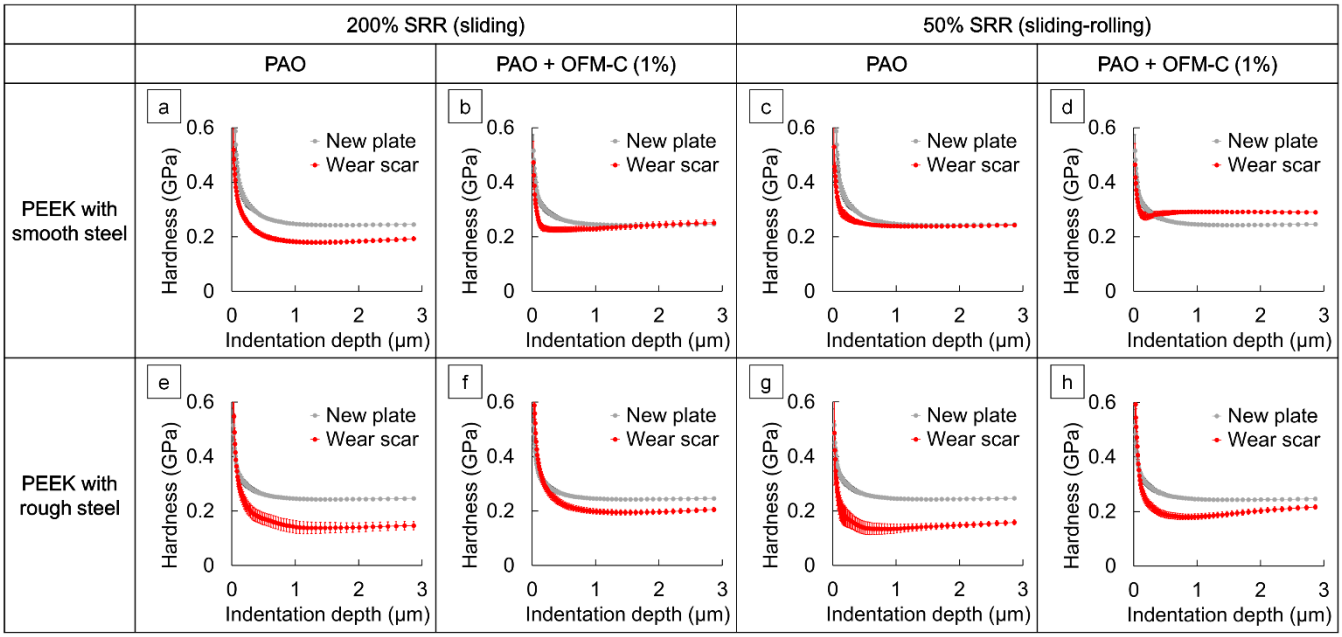
200% SRR (sliding)
50% SRR (sliding-rolling)
PAO
PAO + OFM-C (1%)
PAO
PAO + OFM-C (1%)
PEEK with smooth steel
PEEK with rough steel
a
b
c
d
e
f
g
h
Hardness (GPa)
Indentation depth (μm)
New plate
Wear scar

Fig. 13.

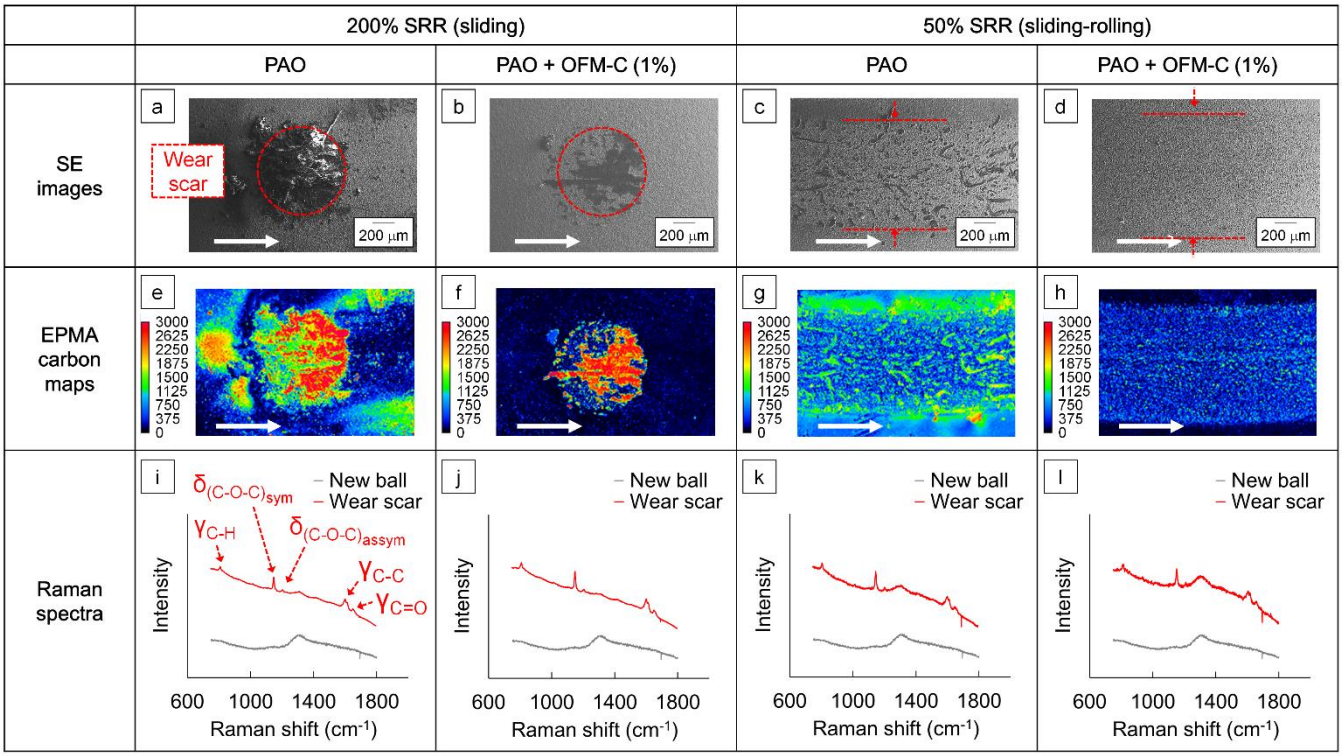
200% SRR (sliding)
50% SRR (sliding-rolling)
PAO
PAO + OFM-C (1%)
PAO
PAO + OFM-C (1%)
SE images
EPMA carbon maps
Raman spectra
Wear scar
200 μm
New ball
Wear scar
Intensity
Raman shift (cm-1)

Fig. 14.

	PEEK – smooth steel				PEEK – rough steel			
	Sliding		Sliding-rolling		Sliding		Sliding-rolling	
	PAO	PAO + OFM	PAO	PAO + OFM	PAO	PAO + OFM	PAO	PAO + OFM
Schematics of contact surfaces	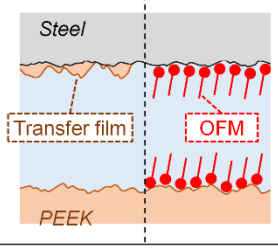		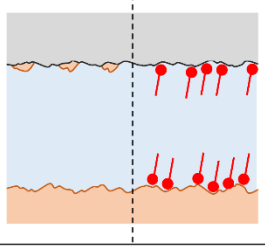		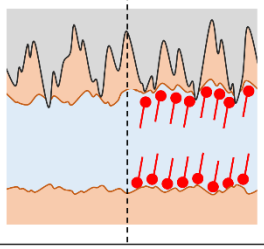		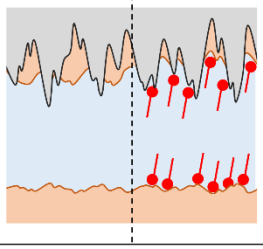	
OFM effect on friction	⬇⬇⬇		⬇⬇		⬇		⬆⬆	
OFM effect on wear	-		-		⬇		⬆⬆	